Catalysis Letters (2019) 149:2279–2290
https://doi.org/10.1007/s10562-019-02807-6

Porous Alkaline-Earth Doped Multiwall Carbon Nanotubes with Base Catalytic Properties

N. Barrios-Bermúdez[1,2] · J. Santos-Granados[3] · V. Calvino-Casilda[4] · A. Cerpa-Naranjo[3] · M. L. Rojas-Cervantes[1]

Received: 11 March 2019 / Accepted: 28 April 2019 / Published online: 4 May 2019

Abstract
Alkaline-earth doped multiwall carbon nanotubes, M-CNT (M = Mg, Ca, Sr, Ba) have been prepared by a combined method of ionic exchange and precipitation. The wide characterization of the solids by nitrogen adsorption, ATR–FTIR, thermal analysis, XRD, scanning electron microscopy, transmission electron microscopy, point of zero charge (PZC), and X-ray photoelectron spectroscopy shows that the incorporation of M to the CNTs has been successfully produced. The doping with the alkaline-earth cations causes a decrease in the S_{BET} value of the raw material, mainly due to the blockage of mesopores by the metal carbonate phase formed in most of cases. This metallic phase also contributes to the destabilization of the nanotubes by promoting their oxidation. According to PZC values, the acid character of oxidized CNTs changes to basic for the M-CNT series, Mg-CNT showing the highest PZC value. The basic properties of the catalysts have been tested in the C–C bond forming reaction of Knoevenagel, by carrying out the condensation of ethyl cyanoacetate with benzaldehyde or 4-methoxybenzaldehyde.

✉ M. L. Rojas-Cervantes
mrojas@ccia.uned.es

[1] Departamento de Química Inorgánica y Química Técnica, Facultad de Ciencias, UNED, Paseo Senda del Rey nº 9, 28040 Madrid, Spain

[2] Departamento de Ciencias, Escuela de Ingeniería, Arquitectura y Diseño, Universidad Europea de Madrid, c/ Tajo s/n, Villaviciosa de Odón, 28670 Madrid, Spain

[3] Departamento de Ingeniería Industrial y Aeroespacial, Escuela de Ingeniería, Arquitectura y Diseño, Universidad Europea de Madrid, c/ Tajo s/n, Villaviciosa de Odón, 28670 Madrid, Spain

[4] Departamento de Ingeniería Eléctrica, Electrónica, Control, Telemática y Química Aplicada a la Ingeniería, ETS de Ingenieros Industriales, UNED, c/ Juan del Rosal 2, 28040 Madrid, Spain

Graphical Abstract

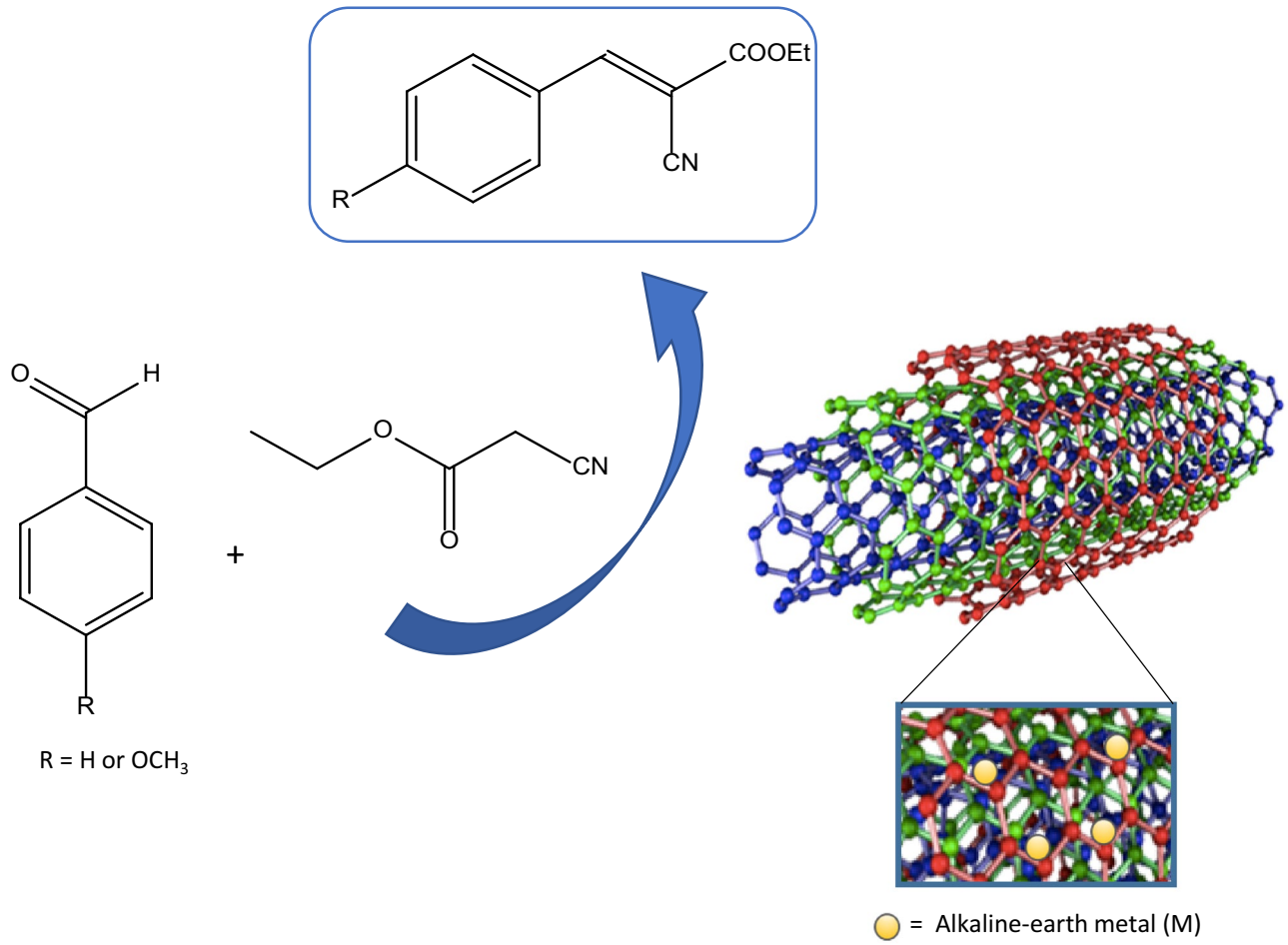

Keywords Alkaline-earth doped carbon nanotubes · Surface and Bulk characterization · Base catalysts

1 Introduction

Carbon nanotubes (CNTs) are fascinating materials [1], with excellent electronic, physical and chemical properties [2, 3], which find interesting applications in the field of catalysis as alternative supports to the conventional ones due to multiple reasons [4–6], among them their high surface active site to volume ratio, light mass density, high porosity, hallow structure and controlled pore size distribution. Additionally, the absence of microporosity eliminates diffusion and interparticle mass transfer, leading to a high accessibility to the active phase. Furthermore, for multiwall CNTs (MWCNTs) their specific surface area and their internal diameter can be tuned according to the catalytic requirement.

In order to be used as catalysts, a wide variety of methods have been applied to deposit the active phase on CNTs [4, 5], thus obtaining decorated CNTs with different metals, mainly transition metals, which can be deposited on their external surface [7, 8], in their inner cavity [9–11], or in both [12]. The choosing of the method depends on the final application of the material, as molecules and nanomaterials on the exterior walls of CNTs display different properties and chemical reactivities from those confined within CNTs.

With the purpose of modifying the acid or basic properties of the CNTs to be used as catalysts different functionalities or heteroatoms can be incorporated. Thus, the basic character can be enhanced by inserting nitrogen functional groups on the CNTs surface or synthesizing them in the presence of a source of nitrogen [13–16]. The blending of CNTs with metal oxides of basic character, such as ZnO, TiO_2, MgO among others [17] also confers basicity to the final material.

Between the reactions catalyzed via basic centres, Knoevenagel condensation has been widely used for the synthesis of key intermediates and final products [18–21]. However, this C–C bond forming reaction and the search for new

materials catalyzing the reaction still arouses great interest in the field of organic synthesis.

In this paper we report by the first time the synthesis of doped alkaline-earth MWCNTs, by ionic exchange between the protons of carboxylic groups of oxidized MWCNTs and the metal chlorides, and subsequent precipitation of the corresponding hydroxides on the walls of CNTs. The characterization of the catalysts by different techniques will allow to identify the influence of the oxidative functionalization, the pyrolysis and the metallic phase incorporated in the nanotubes on their textural and crystalline properties and on their catalytic activity in the Knoevenagel reaction between benzaldehyde (or a substituted benzaldehyde, 4-methoxybenzaldehyde) and ethyl cyanoacetate.

2 Experimental

2.1 Synthesis of the Catalysts

The multiwall carbon nanotubes (named as CNT herein) used as pristine material for the synthesis of the catalysts were provided by Sigma-Aldrich, with the following characteristics: OD × L 6–9 nm × 5 μm and purity > 95%. They were previously functionalized by oxidation with nitric acid, to obtain CNTO sample, according to the procedure described in [22].

The procedure of preparation of alkaline-earth doped CNTs was based on the ionic exchange between the protons of carboxylic groups of CNTO and the metal cations and the subsequent precipitation of the corresponding hydroxides on the walls of CNTs (Scheme 1), and it is detailed as follows. 1 g of CNTO was dispersed in 50 mL of 0.15 M MCl_2 (M = Mg, Ca, Sr, Ba). Ammonium hydroxide was added dropwise until pH 8. The suspension was sonicated for 30 min and then left for 5 h. The solid was filtered, washed until absence of chlorides and dried at room temperature for 24 h and at 60 °C for 16 h. Finally it was pyrolyzed under nitrogen flow of 100 mL/min at 500 °C for 5 h. According to shown in Scheme 1, the initially formed hydroxides must be transformed into the corresponding oxides; however, the metal carbonate phases are also formed, as it will be seen below by XRD results. It is supposed that some atmospheric CO_2 held in the pores of the catalyst structure could be catched by the surface oxide groups, leading to the formation of carbonates, in spite of the fact that the pyrolysis was carried out under inert atmosphere. The catalysts thus obtained were denoted as M-CNT (with M = Mg, Ca, Sr, Ba). For comparison, the oxidized nanotubes without doping treatment were also pyrolyzed in the same conditions, obtaining the CNTOp sample.

2.2 Characterization of the Catalysts

The textural properties of samples were determined from the nitrogen adsorption–desorption isotherms at − 196 °C, by using a Micromeritics ASAP 2010 equipment. The samples were previously outgassed at 150 °C for 8 h until a vacuum set point of 200 μm Hg. The surface area and micropore volume were determined by BET method and *t*-plot method,

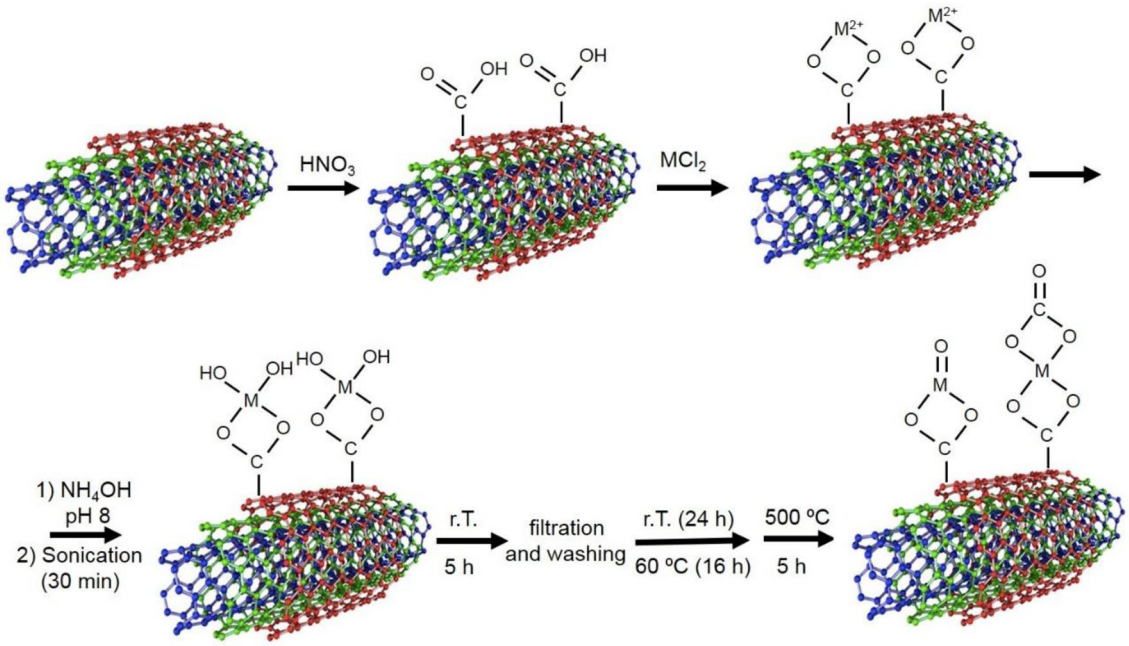

Scheme 1 Schematic illustration of the procedure for preparation of M-CNT samples

respectively, and the mesoporosity characteristics of samples were obtained by the BJH method. A Seiko SSC 5200 TG–DTA 320 System was used for the thermal analysis of samples, by heating about 20 mg of sample in air flow of 100 mL/min from 30 up to 1000 °C (heating rate of 10 °C/min). Infrared spectra of CNT, CNTO, CNTOp and M-CNT samples were measured in a FT-IR Nicolet iS50 (Thermo Scientific) instrument, equipped with ATR analyzer of germanium in the 4000–700 cm^{-1} range. Transmission electron microscopy (TEM) images of the samples were recorded by using a JEOL 2100 microscope operating at 200 kV and scanning electron microscopy (SEM) and energy dispersive X-ray spectroscopy (EDX) measurements were performed using an Oxford Instrument, model: X-Max of 80 mm^2 and resolution between 127 eV and 5.9 keV. X-ray diffraction patterns were registered using a X'Pert Pro Panalytical diffractometer with Cu Kα radiation (1.5406 Å), operating at 40 kV and 40 mA.

The surface chemical composition was analyzed by X-ray photoelectron spectroscopy (XPS). The spectra were obtained on a SPECS GmmH spectrometer equipped with a PHOIBOS 150 9MCD hemispherical multichannel electronics analyzer. The pressure in the analysis chamber was kept below 8×10^{-10} mbar and the excitation source was the Al Kα line ($h\nu = 1486.74$ eV, 12 kV, 200 W). The binding energy was referenced to the C1s line at 284.6 eV.

The point of zero charge (PZC) was measured following a similar procedure to that described in [23], with some modifications. Twelve solutions in the range of pH 1.0–12.0 were prepared using dilute aqueous solutions of NaOH and HCl and $NaNO_3$ as electrolyte. A 4.5 mL aliquot of each solution was pipetted into polyethylene vials and allowed to equilibrate for 1 h. The initial pH of each solution was then recorded. A 5.0 mg amount of the CNTs were added to each vial, which was then capped, sealed and stirred for 24 h. Afterwards, the solid was removed by filtration and the final pH of the solution was measured. The plateaus of the plots of initial versus final pH values reveal the PZC value for each sample.

2.3 Catalytic Activity

Knoevenagel condensation between an aldehyde (benzaldehyde or 4-methoxybenzaldehyde) and ethyl cyanoacetate was carried out under inert atmosphere in absence of solvent by mixing equimolar amounts of both reactants (14 mmol of each) in a three-necked reactor on a StarFish multi-experiment work station, equipped with thermometer. After equilibrating the reactants at 90 °C, the catalyst was added. The amount of catalysts used was 1 wt% when benzaldehyde was condensed, and 1 and 2 wt% in the case of 4-methoxybenzaldehyde. The samples taken periodically from the batch reactor at selected reaction times were filtered to remove the catalyst and analyzed by gas chromatography in an Agilent 6890 GC equipment. Once the reaction was finished, tests of recyclability of the catalysts were carried out. For this, the catalyst was filtered, washed with acetone several times and dried at 100 °C for 24 h before to be reused in a new cycle of reaction. As a result of the slight loss of catalyst amount produced between consecutive cycles, it was necessary to rescale the amount of reactants in order to keep constant the catalyst/reactants ratio.

3 Results and Discussion

3.1 Physicochemical Characterization

Figure 1 shows the diffraction patterns of CNT, CNTO and CNTOp samples. The peaks observed at $2\theta = 25.8°$ and 43° in the diffractogram of commercial CNT (Fig. 1a) can be assigned to hexagonal graphite (JCPDS-ICDD 01-075-1621), and two peaks of low intensity placed at $2\theta = 14.8°$ and 31° are associated with $CoCu_2Sn$ (JCPDS-ICDD 00-029-0467), present as metallic impurities derived from the preparation method. This impurity disappears after the treatment with nitric acid (see the corresponding diffraction patterns of CNTO and CNTOp samples). The crystallite size of graphite calculated determined according to Scherrer equation was similar for the three samples, around 3.2–3.5 nm.

After doping with the alkaline-earth chlorides and pyrolysis of the oxidized nanotubes, the presence of metal carbonates is detected (see Fig. 1b). Although it cannot be discarded that metal oxides are formed initially, they must be transformed into the corresponding carbonates. Thus, the phases corresponding to $CaCO_3$ (JCPDS-ICDD 00-002-0629, crystallite size of 28.2 nm), $SrCO_3$ (JCPDS-ICDD 00-005-0418, crystallite size of 8.7 nm), and $BaCO_3$ (JCPDS-ICDD 00-041-0373, crystallite size of 12.5 nm) are present in the Ca-CNT, Sr-CNT and Ba-CNT samples, respectively. However, in the diffractogram of Mg-CNTO, no metallic phase is detected. The slightly lower percentage of Mg incorporated (as determined by TG analysis, see below) may be responsible for a higher dispersion and the formation of crystallite size lower than 4 nm, not being detected by XRD technique. The doping with the alkaline-earth cations does not affect the crystallinity of graphite from nanotubes, as the crystallite size of this phase in M-CNTO samples was barely modified, being around 3.0–3.3 nm.

In order to quantify the amount of alkaline-earth metal incorporated to the oxidized nanotubes and to study its influence on their thermal stability, thermogravimetric analysis of pyrolyzed nanotubes were carried out in air. The final residue obtained together with the range of decomposition temperature of CNTs are given in Table 1.

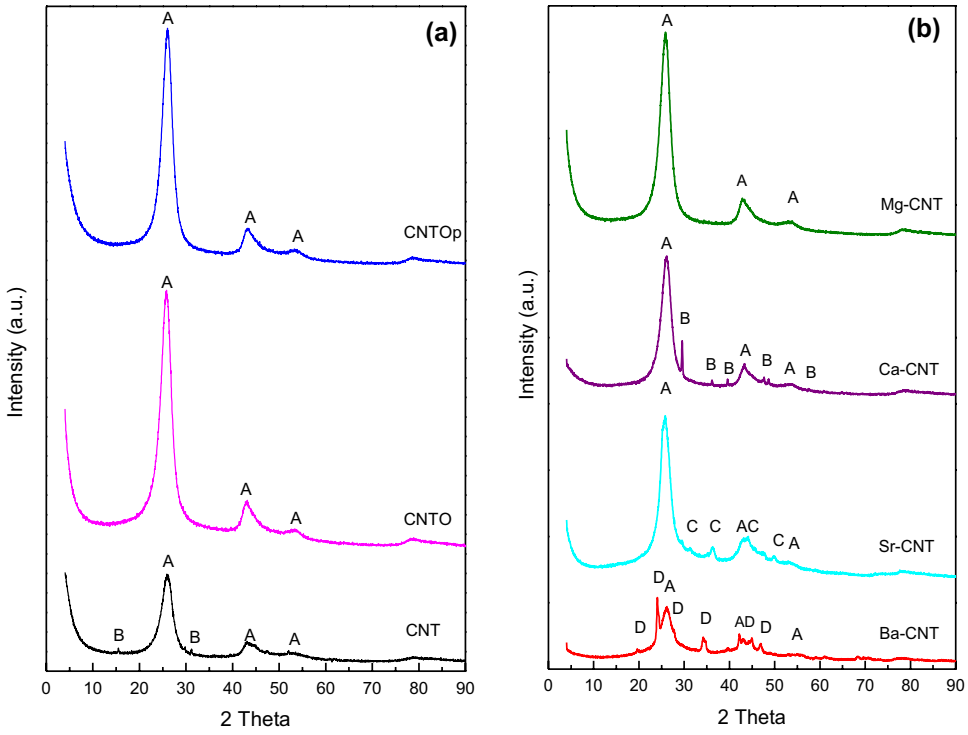

Fig. 1 XRD patterns of carbon nanotubes. **a** CNT, CNTO and CNTOp and **b** M-CNT (M = Mg, Ca, Sr, Ba). *A* graphite, *B* $CaCO_3$, *C* $SrCO_3$, *D* $BaCO_3$

Table 1 Temperatures of decomposition of carbon nanotubes (T_{dec}), residues and metal amount of the samples determined by thermal analysis in air

Samples	T_{dec} (°C)	Residue (wt%)	MO (%)	M (%)	at-g M/100 g
CNTOp	400–640	0.56	–	–	–
Mg-CNT	350–590	4.0	3.44	2.1	0.086
Ca-CNT	325–590	6.36	5.80	4.12	0.103
Sr-CNT	315–540	11.1	10.54	12.43	0.102
Ba-CNT	290–500	14.9	14.34	12.8	0.093

Notice that the oxidation process of the nanotubes occurs in the M-CNT samples at a lower temperature than that of CNTOp, around 50 °C lower in the case of Mg-CNT, 100 °C for Ca-CNT and Sr-CNTO, and 140 °C for Ba-CNT, suggesting that the metallic phase contributes to the destabilization of the nanotubes by promoting their oxidation, according to previous results found by us [22]. Furthermore, in general, these results are in agreement with those reported for MWCNTs by other authors, who found that the lower the metallic content, the higher the oxidation temperature was [24]. The final residue obtained for M-CNT, higher than that for CNTOp (see Table 1), confirms the incorporation of the alkaline-earth metal to the nanotubes. By assuming that the final residue corresponds to the content in oxide MO, the amounts of incorporated metal were calculated. Although the wt% of metal increases with the cation size, when transformed in terms of at-g M/100 g sample, it is observed that the alkaline-earth cations have been exchanged in a similar amount, around 0.100 at-g/100 g, although the Mg has been incorporated in less extent.

From the textural properties of the samples (Table 2), it can be seen that CNTs under study are mesoporous solids, as deduced from the values of V_{mes} and V_{mic}, and the major contribution to the porosity proceeds mainly from the void space between the bundles, which results in lower surface areas compared to other carbon materials. The commercial CNT shows a mesopore volume (2–50 nm) of 0.530 cm^3/g and a specific surface area of 248 m^2/g, which is very similar to that reported by other authors for other commercial MWCNTs [25–27]. As observed in Table 2, a slight increment in the BET surface area and pore volume is produced after oxidation of CNT (compare values for CNT and CNTO), similarly to that reported previously [26, 27], due to the removal of amorphous carbon and impurities of the surface [28, 29] and to a shortening of the nanotubes [30]. The pyrolysis of the oxidized nanotubes leads to the removal of the oxygen functionalities anchored to the walls of nanotubes, producing a development of mesoporosity (compare V_{mes} values for CNTO and CNTOp, Table 2).

When the CNTO are doped with the alkaline-earth metals, the S_{BET} values decrease, this decrease being higher as bigger the size of the cation. The diminishment in the surface areas values is mainly due to the blockage of mesopores (compare V_{mes} for the M-CNTO series with that of CNTOp) by the metallic carbonate, whose crystallite sizes, determined by Scherrer equation, are in the order of mesopore

Table 2 Textural characteristics and PZC values of the samples

	S_{BET} (m^2/g)	S_{mic} (m^2/g)	V_p (cm^3/g)	V_{mic} (cm^3/g)	V_{mes} (cm^3/g)	d_{mes} (nm)	PZC
CNT	248.0	24.7	0.799	0.012	0.518	12.9	6.4
CNTO	259.9	15.9	0.964	0.008	0.756	18.6	2.6
CNTOp	313.2	12.6	1.072	0.007	0.859	15.7	4.8
Mg-CNT	240.0	5.6	0.948	0.003	0.772	16.6	9.8
Ca-CNT	215.4	0.4	0.873	0.001	0.699	17.5	9.1
Sr-CNT	214.9	–	0.934	–	0.749	18.5	8.9
Ba-CNT	187.5	9.5	0.906	0.005	0.712	19.5	9.0

S_{BET} specific surface area, S_{mic} micropore surface area determined by *t*-plot, V_p pore volume at single point at $P/P_0 = 0.967$, V_{mic} micropore volume by *t*-plot method, V_{mes} mesopore volume by BJH between 2 and 50 nm, d_{mes} average mesopore diameter (4V/A) by BJH, *PZC* point of zero charge values

sizes (see results above). However, a blockage of micropores is also produced, as deduced by the values of V_{mic}, being more accused for Ca-CNT and Sr-CNT, especially for this last sample. The decrease in the S_{BET} and V_{mes} values is less accused in the case of Mg-CNT, for which, according to the TG analysis, a less amount of metal has been anchored to the nanotubes.

The ATR–FTIR spectra for CNT, CNTO and CNTOp samples are displayed in Fig. 2a. A band centred at 1550 cm^{-1}, assigned to –C=C– vibrations of the skeleton of CNT [31, 32] is observed in all cases. The presence of carboxylic groups in the CNTO and CNTOp is corroborated by the band centred at 1715 cm^{-1}, assigned to C=O stretching [31, 33] and the band around 1160 cm^{-1}, associated with C–O stretching vibrations [32, 34]. The partial removal of these groups after pyrolysis is confirmed by the decreasing in the intensity of both bands in the spectrum of CNTOp, with respect to that of CNTO. The band placed at 1850 cm^{-1} in the spectrum of CNTO can be due to the symmetric stretching of carbonyl groups in anhydride structures [35] and that located at 1050–1060 cm^{-1} can be assigned to =C–O–C stretching vibrations in ether functionalities [32].

In the infrared spectra of the alkaline-earth doped nanotubes (Fig. 2b), the appearing of new bands and the shift of the existing ones in the spectrum of CNTOp occurs, as a result of the interaction between the alkaline-earth metals and the walls of nanotubes. In this sense, two bands associated with carbonate groups are observed in the spectra of Ba-CNT, Sr-CNT and Ca-CNT (for these samples, the corresponding alkaline-earth carbonates were detected by XRD). For Ba-CNT, a very intense band placed at 1420 cm^{-1} can be associated with antisymmetric stretching of the carbonate groups and the band of lower intensity located at 850 cm^{-1} could be due to the out-of-plane bend of the same group [35]. These bands are also present in the spectra of Sr-CNT and Ca-CNT, although with lower intensity. The band placed at 1060 cm^{-1} in the spectrum of Ba-CNT could be associated, as explained above, with =C–O–C stretching vibrations in ether functionalities [32]. Finally, the bands at

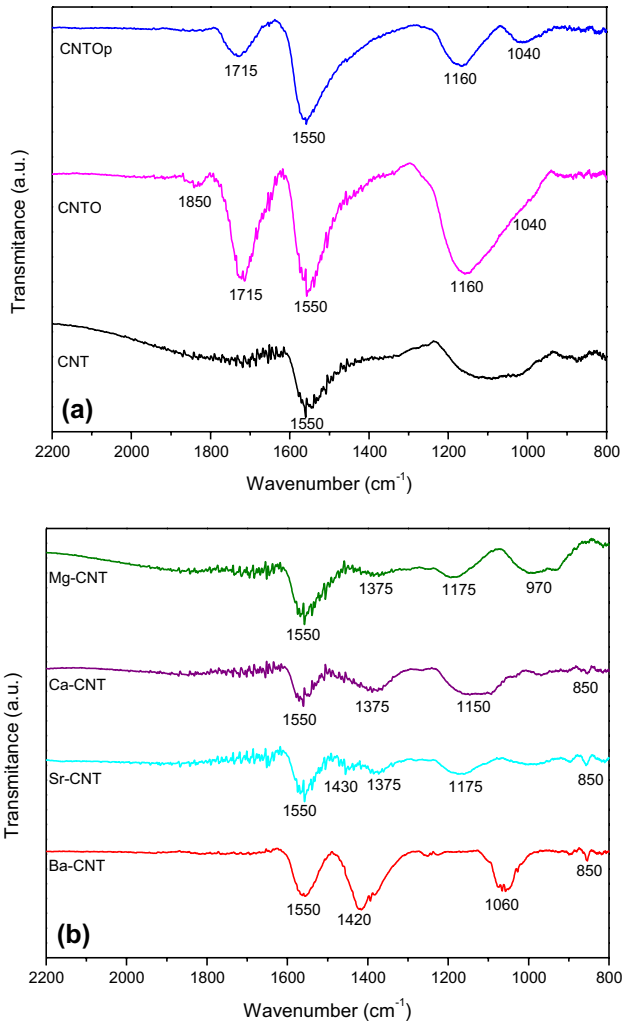

Fig. 2 ATR–FTIR spectra of **a** CNT, CNTO and CNTOp and **b** M-CNT (M = Mg, Ca, Sr, Ba)

1150–1175 cm^{-1} and 1375 cm^{-1} in the spectra of M-CNT samples could be assigned to antisymmetric stretching of O–C–C groups and antisymmetric stretching of CO–O groups, respectively, present in esters and lactones [36].

Considering that catalytic reactions are mostly carried out at the surface of the solids, composition of surface of the catalysts was analysed by XPS. The atomic composition (%) is given in Table 3. It can be seen that the oxidation process of pristine CNTs was successfully produced, as deduced from the increment in oxygen content from 2.3% (for CNT) to 22% (for CNTO). Some of these oxygen groups incorporated during oxidation are removed after pyrolysis (12.6% oxygen for CNTOp) and in the doped samples. Notice that the surface is significantly enriched in alkaline-earth cations with respect to the bulk (compare results of at.% M of Table 3 with those of at-g M/100 g in Table 1). With the exception of Mg-CNT, the presence of chloride is detected at the surface of the doped CNTs, which can remains as a residue, resulting from the synthesis process, even though the samples were washed repeatedly.

The morphology and surface element composition were observed by TEM and SEM–EDX. Figure 3 shows the TEM spectra of samples and their corresponding EDX analysis. The cylindrical structure of nanotubes (with a diameter of 6–9 nm, according to data of manufacturer) is clearly observed in all cases. The oxidation causes the partial rupture of some nanotubes and the opening of the tips, as can be seen in the zones marked with red circles in Fig. 3b, i. The incorporation of alkaline-earth metals produces the creation of some defects and irregularities over the walls of nanotubes (Fig. 3g, e, zones with red circles). The corresponding EDX spectra show the presence of the alkaline-earth elements, indicating that their incorporation to the CNTs has occurred. The presence of these elements in the CNTs is also corroborated by checking the EDX spectra of the SEM images (Fig. 4), obtained from central area of images, where the corresponding atomic percentages are also given. The at.% values are similar and of the same order of magnitude to those obtained by XPS analysis (see Table 3), with the exception of Ca-NTC, for which a value of almost ten times higher is obtained by EDX analysis.

From the PZC values of the samples (Table 2), it is deduced that the almost neutral character of the surface (PZC = 6.4) of commercial CNT, changes to acid (PZC of 2.6 for CNTO sample) due to the presence of some oxygenated groups, mainly carboxylic groups, after treatment with nitric acid. The removal of most of these oxygenated groups by pyrolysis produces an increment in PZC valued (4.8 for CNTOp). For M-CNT samples, the PZC values are much higher (PZC ≥ 9) than for CNTO, which proves the anchoring of the alkaline-earth metals to the surface of nanotubes, the presence of carbonate species conferring basic character to the CNT surface. With the exception of Mg, which shows the highest basicity (PZC = 9.8), the PZC values for the M-CNTO samples are very similar, around 9.0.

Table 3 Surface concentrations (at.%) of the samples determined by XPS

	C	O	M	Cl
CNT[a]	97.3	2.35	–	–
CNTO	78.0	22.0	–	–
CNTOp	87.4	12.6	–	–
Mg-CNT	92.28	6.48	1.24	–
Ca-CNT	86.7	10.91	2.17	0.22
Sr-CNT	92.7	6.44	0.72	0.14
Ba-CNT	91.8	6.8	1.20	0.20

[a]For this sample, 0.35% of sulphur was detected

3.2 Catalytic Activity

The conversion values of benzaldehyde (%) in the condensation with ethyl cyanoacetate over M-CNT catalysts (Fig. 5) reveal that the reaction proceeds effectively when alkaline-earth cations are anchored to the walls of nanotubes, in contrast to CNT and CNTO samples, which resulted in a negligible activity (not shown in Fig. 5).

The conversion of benzaldehyde for all the M-CNT samples increased with the reaction time, as expected. Ethyl(2E)-2-cyano-3-phenyl-2-propenoate was the only reaction product obtained in all cases. Conversion values comprised between 64 and 85% were reached after 240 min. The order of catalytic activity observed at higher reaction times was: Ca < Sr < Ba ≅ Mg. Considering that the amount of metal incorporated for the first three catalysts, and therefore, the amount of basic centres, was similar in all cases (see values of number of at-g M/100 g sample, Table 1), the activity order seems to be in agreement with the increment in the basic character of the corresponding carbonate (phase detected by XRD) when descending in the group of alkaline-earth metals. However, the activity of Mg-CNT, for which less amount of metal was incorporated, was very similar to that of Ba-CNT after 120 min of reaction, being the most active catalyst at low reaction times. The activity of Mg-CNT, higher than the expected according to the basic character of the metal, could be caused by a higher dispersion of the active phase, resulting in smaller particles, not being detected by XRD. The unexpected higher activity of Mg-CNT could also be explained by the fact that for this catalyst no chloride was detected at the surface, in contrast to the observed for the rest of samples. May be these chloride ions can poison or inhibit some of the active sites of the M-CNT (M = Ca, Sr, Ba) catalysts, which should result in a higher activity of Mg-CNT.

Ca-NTC and Sr-NTC are less active than the rest of catalysts. This could be due to the fact that, for these samples, not all of the metallic active centres are placed in the mesopores, but some of them could be located in the micropores, blocking them (these two samples have the lowest V_{mic} values,

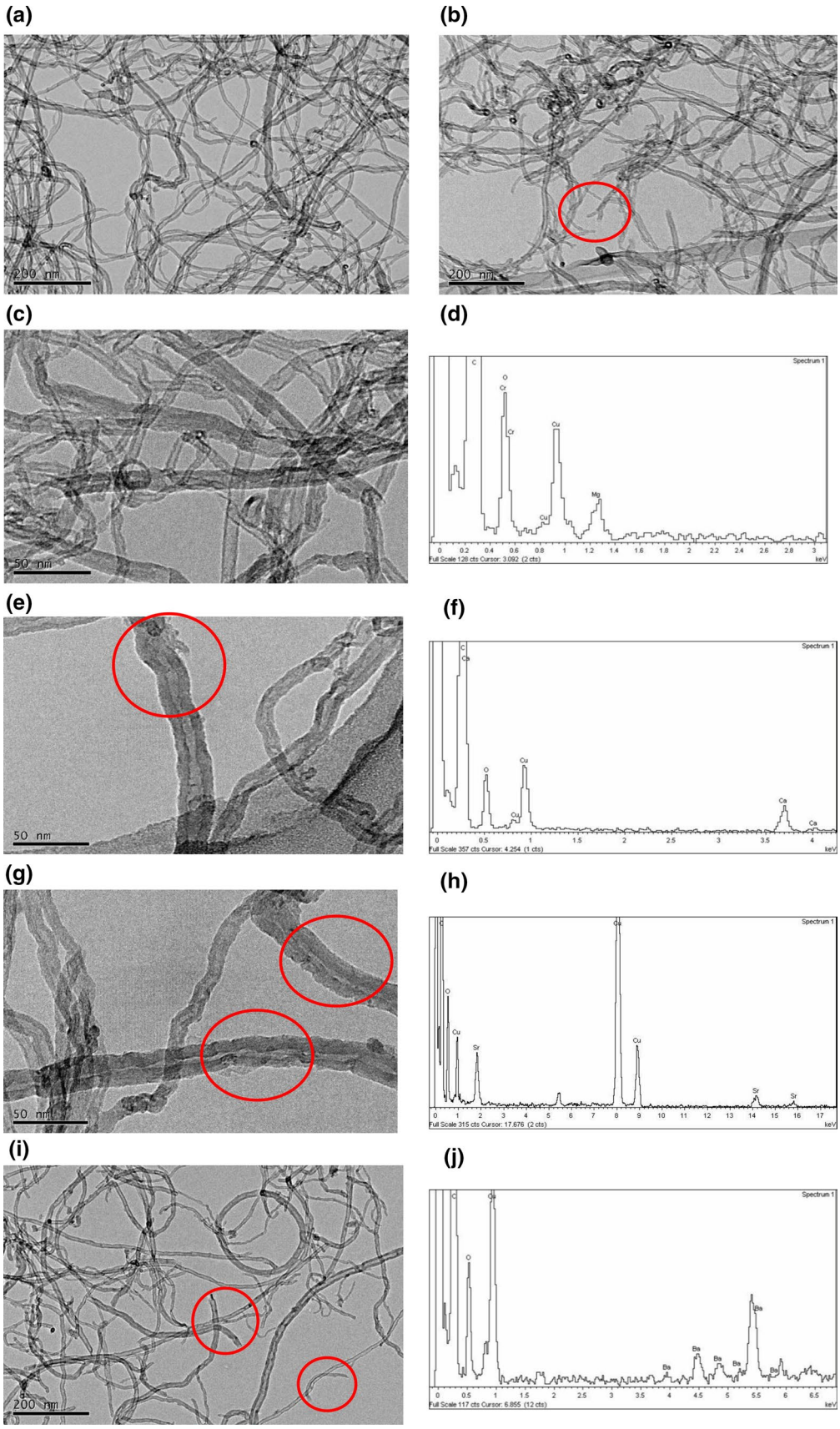

Fig. 3 TEM spectra of samples and their corresponding EDX analysis. **a** CNTO, **b** CNTOp, **c** and **d** Mg-CNT, **e** and **f** Ca-CNT, **g** and **h** Sr-CNT, **i** and **j** Ba-CNT

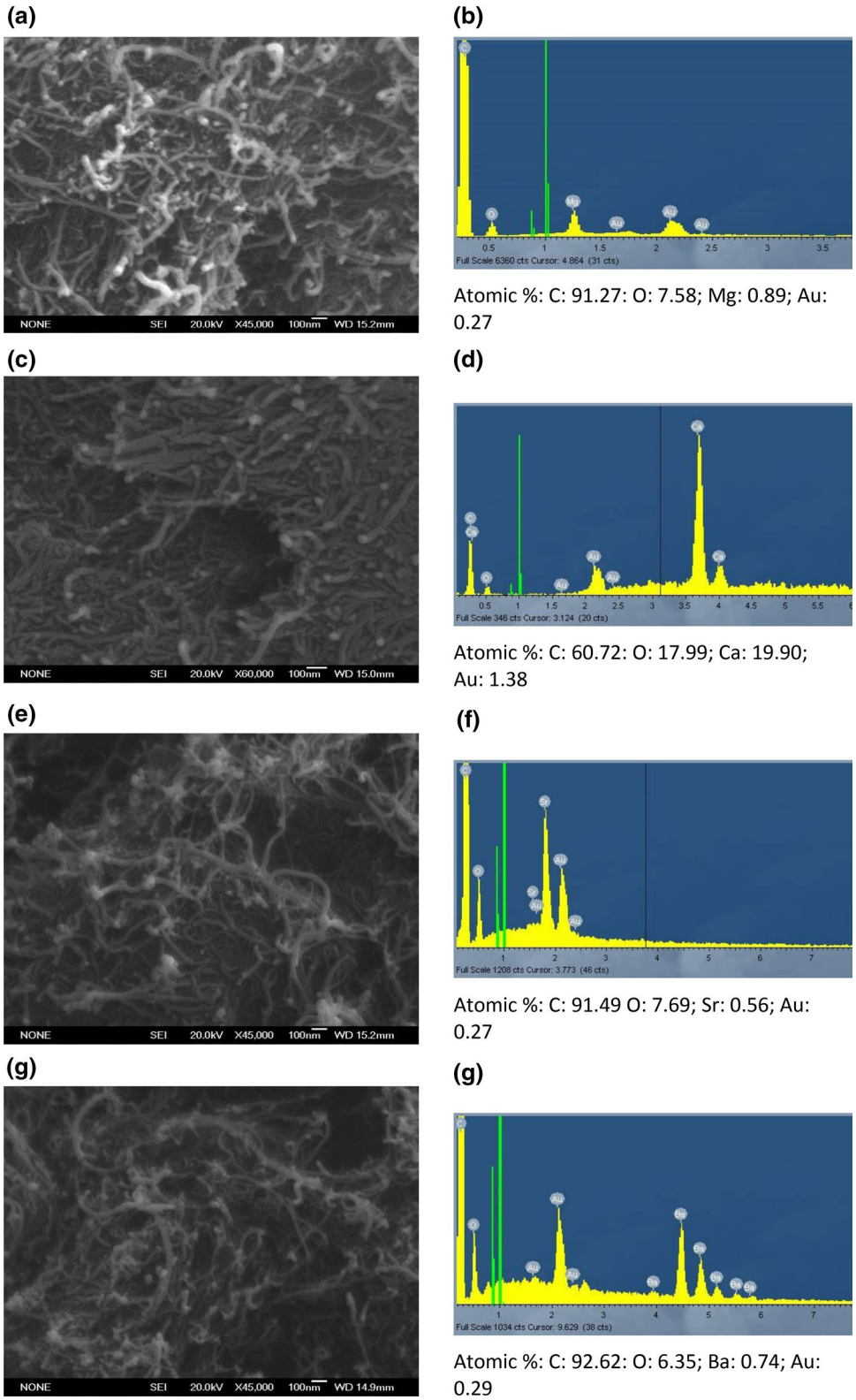

Fig. 4 SEM microphotographs and their corresponding EDX spectra. **a** and **b** Mg-CNT, **c** and **d** Ca-CNT, **e** and **f** Sr-CNT, **g** and **h** Ba-CNT

Table 2), being more difficult for the Knoevenagel reactants to access to them. Therefore, although the catalytic activity seems to depend mainly on the basic character of the alkaline-earth cation and the amount of these basic centres incorporated to the CNTs, the influence of the textural properties cannot be discarded. This influence of the porous structure on the catalytic behaviour in Knoevenagel condensation has been also reported for other materials [37, 38].

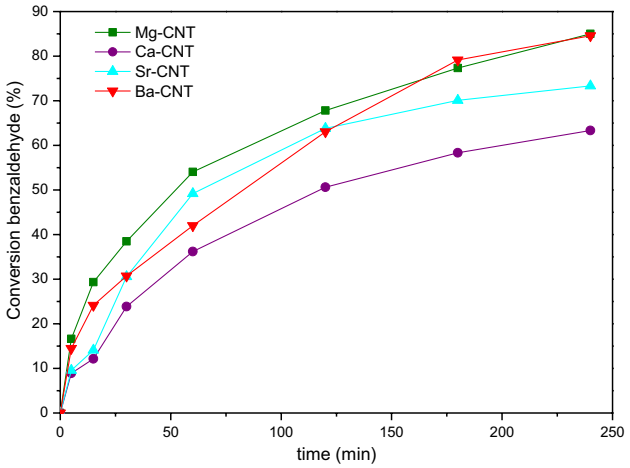

Fig. 5 Knoevenagel reaction between benzaldehyde and ethyl cyanoacetate over M-CNTOM (M = Mg, Ca, Sr, Ba) catalysts at 90 °C

With the aim of comparing with other data from literature, the values of catalytic activity for the Knoevenagel condensation ($pK_a = 9$) were expressed in terms of yields (mol/g_{cat} h). The values of yields obtained at 60 min, were 0.252 mol/g h for Mg-NTC, 0.169 mol/g h for Ca-NTC, 0.230 mol/g h for Sr-NTC, and 0.197 mol/g h for Ba-NTC. These values are remarkably higher than those obtained by other authors, 0.045 mol/g h in [39] and 0.017 mol/g h in [40], when using nitrogen-doped CNTs at 80 °C at the same reaction time and similar reaction conditions, which proves the efficiency of our catalysts for this reaction.

Some experiments of recycling of the catalysts were carried out in order to determine their stability. Figure 6 shows the conversion values after 240 min of reaction for four consecutive cycles. Notice that the most stable catalyst was Ca-CNT, for which a decrease of 10% in the conversion values is produced after four cycles. However, for the rest of samples, a more accused diminishment in the activity was observed, being comprised between the 22% for Mg-CNT and the 30% for Sr-CNT. It has to be remarked that in general the most significant decrease in the activity occurs from the first to the second cycle, which could be due to a leaching of the alkaline-earth metals to the solution or by a deactivation of the active sites due to the adsorption of the organic products on them. However, the activities for the successive cycles were similar, the deactivation for the second to fourth runs being quite lower.

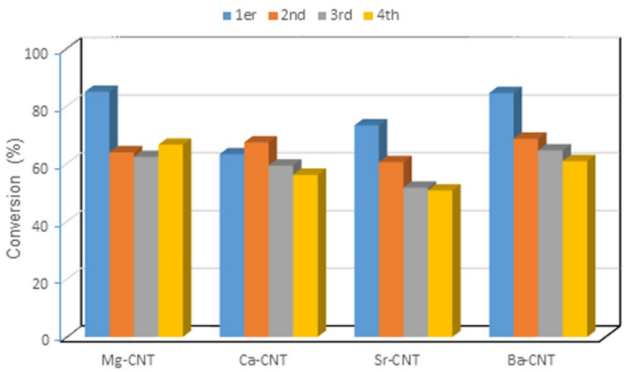

Fig. 6 Recyclability of the catalysts in the Knoevenagel reaction between benzaldehyde and ethyl cyanoacetate at 90 °C. Reaction time 4 h

In order to study the influence of a substituent in the aldehyde molecule in the Knoevenagel reaction, this was carried out by condensation between ethyl cyanoacetate and a substituted benzaldehyde, 4-methoxybenzaldehyde. The conversion values of 4-methoxybenzaldehyde, which contains an electron donor group in 4-position, are shown in Fig. 7a.

It can be noticed that the conversion values of 4-methoxybenzaldehyde were lower than those of benzaldehyde. Mg-CNT was again the most active of the catalysts (conversion

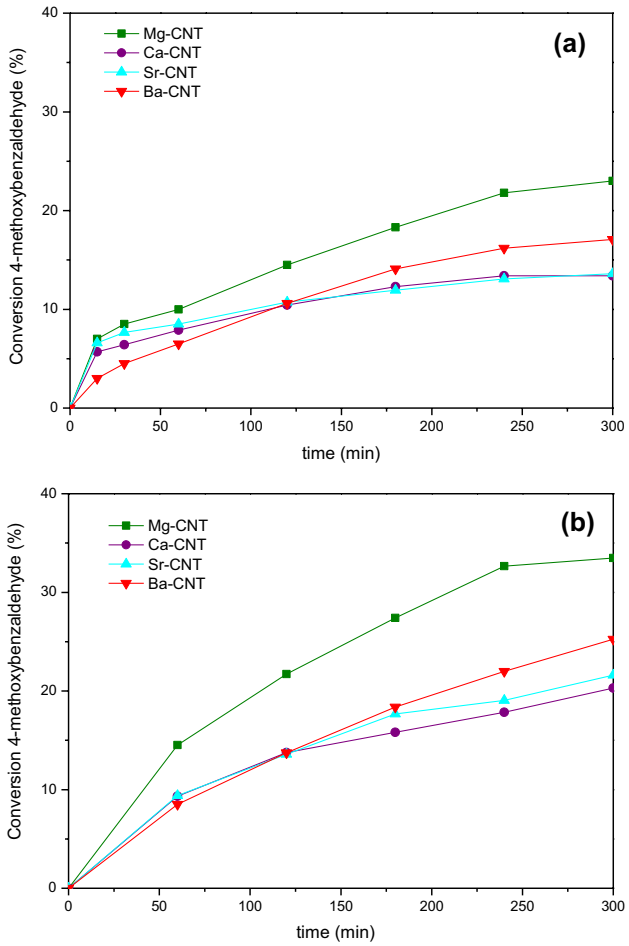

Fig. 7 Knoevenagel reaction between 4-methoxybenzaldehyde and ethyl cyanoacetate over M-CNTOM (M = Mg, Ca, Sr, Ba) catalysts at 90 °C. **a** 1 wt% catalyst and **b** 2 wt% catalyst

of 22% at 240 min), and the trend of catalytic activity was similar to that observed for benzaldehyde, leading to conversion values comprised between 13.6% for Ca-CNT and 17% for Ba-CNT after 300 min of reaction. The Knoevenagel condensation product was the only one detected in all cases, resulting in a total selectivity. The non-catalyzed reaction led to conversion values of only 4% after 300 min, therefore the introduction of alkaline-earth metals into the CNTs results in active catalysts for the Knoevenagel condensation. The mechanism for the Knoevenagel condensation over acid, basic, and acid–base sites is very well reported [37, 38]. In the M-CNT catalysts, the basic active centres abstract an alpha proton from the methylene carbon in ethyl cyanoacetate forming a carbanion. The basic centres also form a carbocation on the benzaldehyde carbon. Then, the carbanion interacts with the carbocation towards the Knoevenagel product. The attack of the carbanion on benzaldehyde carbon atom (carbocation) requires the accessibility to this carbon atom. In case of benzaldehyde, this carbon atom is more accessible than in 4-methoxybenzaldehyde and therefore M-CNT catalysts were more active. In case of the 4-methoxybenzaldehyde molecule the access to this carbon atom can be sterically congested and influenced in the neighborhood by the 4-methoxy substituent resulting in a lower activity. In order to achieve higher activities the amount of catalyst was duplicated. The results (Fig. 7b) show that the conversion values were not duplicated but multiplied by a factor between 1.3 and 1.6 when the amount of catalyst increased from 1 to 2 wt%. Again, Mg-CNT was the most active catalyst, leading to a conversion value of 34% at 300 min, while the other three catalysts showed similar conversion curves at all the reaction times, reaching final conversion values between 21 and 25%.

4 Conclusions

CNTs doped with alkaline-earth metals have been successfully prepared, as determined by different characterization techniques, by an ionic exchange–precipitation method starting from commercial CNTs oxidized and the corresponding metal chlorides. The alkaline-earth cations have been exchanged in a similar amount, around 0.100 at-g/100 g, although the surface of catalysts is significantly enriched in them with respect to the bulk. The S_{BET} values of M-CNT samples decrease with respect to that of non-doped nanotubes, mainly due to the blockage of mesopores by the metal carbonate (phase detected by XRD and FTIR–ATR) formed after pyrolysis in most of cases. The basic character of the samples (as deduced from PZC values) has been tested in the Knoevenagel condensation between ethyl cyanoacetate and benzaldehyde or 4-methoxybenzaldehyde. Conversion values comprised between 64 and 85% were obtained after 240 min when the reaction was carried out with benzaldehyde, Mg-CNT being the most active catalyst. Studies of recyclability showed that Ca-CNT was the most stable sample, for which a decrease of 10% in the conversion values was produced after four cycles. The catalytic activity seems to depend mainly on the basic character of the alkaline-earth cation and the amount of these basic centres incorporated to the CNTs; however, the influence of the textural properties cannot be discarded, as the presence of some of the metals into the micropores makes more difficult the access of the reactants to them. These alkaline-earth CNTs could be applied as catalysts in other C–C bond forming reactions requiring basic character.

Acknowledgements This work was supported by the Spanish Ministry of Science and Innovation (CTM2014-56668-R) and by 2017/UEM09.

Compliance with Ethical Standards

Conflict of interest The authors declare that they have no conflict of interest.

References

1. Harris PJF (2009) Carbon nanotube science: synthesis, properties and applications. Cambridge University Press, New York
2. Baughman RH, Zakhidov AA, de Heer WA (2002) Science 297:787
3. O'Connell M (2006) Carbon nanotubes: properties and applications. Taylor and Francis, Boca Raton
4. Serp P, Corrias M, Kalck P (2003) Appl Catal A 253:337
5. Serp P, Castillejos E (2010) ChemCatChem 2:41
6. Melchionna M, Marchesan S, Prato M, Fornasiero P (2015) Catal Sci Technol 5:3859
7. Wu X-M, Guo Y-Y, Zhou J-M, Lin G-D, Dong X, Zhang H-B (2008) Appl Catal A 340:87
8. Zhang L, Wen G, Liu H, Wang N, Su DS (2014) ChemCatChem 6:2600
9. Zhang H, Pan X, Bao X (2013) J Energy Chem 22:251
10. Pan X, Bao X (2011) Acc Chem Res 44:553
11. Grossmann D, Dreier A, Lehmann CW, Gruenert W (2015) Microporous Mesoporous Mater 202:189
12. Wang X, Li N, Pfefferle LD, Haller GL (2013) Microporous Mesoporous Mater 176:139
13. Ramirez-Barria C, Guerrero-Ruiz A, Castillejos-Lopez E, Rodriguez-Ramos I, Durand J, Volkman J, Serp P (2016) RSC Adv 6:54293
14. Van Dommele S, Romero-Izquierdo A, Brydson R, de Jong KP, Bitter JH (2008) Carbon 46:138
15. Faba L, Criado YA, Gallegos-Suarez E, Perez-Cadenas M, Diaz E, Rodriguez-Ramos I, Guerrero-Ruiz A, Ordonez S (2013) Appl Catal A 458:155
16. Arrigo R, Havecker M, Wrabetz S, Blume R, Lerch M, McGregor J et al (2010) J Am Chem Soc 132:9616
17. Zapata PA, Faria J, Pilar Ruiz M, Resasco DE (2012) Top Catal 55:38
18. Chaudhari BR (2016) World J Pharm Res 5:1644
19. Ebitani K (2014) Comprehensive organic synthesis, 2nd edn. Elsevier B.V., Oxford, pp 571–605

20. Hu X-M, Zhao Y, Gao Y-F, Xiao Y-B, Zhang B-X (2012) Adv Mater Res 554–556:557
21. Bigi F, Quarantelli C (2012) Curr Org Synth 9:31
22. Delgado-Gomez FJ, Calvino-Casilda V, Cerpa-Naranjo A, Rojas-Cervantes ML (2017) Mol Catal 2017(443):101
23. McPhail MR, Sells JA, He Z, Chusuei CC (2009) J Phys Chem C 113:14102
24. Singh DK, Iyer PK, Giri PK (2009) J Nanosci Nanotechnol 9:5396
25. Delidovich I, Palkovits R (2016) Microporous Mesoporous Mater 219:317
26. Dominguez C, Perez-Alonso FJ, Abdel Salam M, Al-Thabaiti SA, Obaid AY, Alshehri AA et al (2015) Appl Catal B 162:420
27. Nowicki P, Szymanowski W, Pietrzak R (2015) Pol J Chem Technol 17:120
28. Ebbesen TW, Hiura H, Bisher ME, Treacy MMJ, Shreeve-Keyer JL, Haushalter RC (1996) Adv Mater 8:155
29. Osswald S, Havel M, Gogotsi Y (2007) J Raman Spectrosc 38:728
30. Ovejero G, Sotelo JL, Romero MD, Rodriguez A, Ocana MA, Rodriguez G et al (2006) Ind Eng Chem Res 45:2206
31. Zhang J, Zou H, Quan Q, Yang Y, Li Q, Liu Z et al (2003) J Phys Chem B 107:3712
32. Goyanes S, Rubiolo GR, Salazar A, Jimeno A, Corcuera MA, Mondragon I (2007) Diam Relat Mater 16:412
33. Chen S, Shen W, Wu G, Chen D, Jiang M (2005) Chem Phys Lett 402:312
34. Wei L, Zhang Y (2007) Chem Phys Lett 446:142
35. Kennet A, Rubinson JFR (2001) Análisis Instrumental Spanish edition, 1st edn. Pearson Publications Company, London
36. Pretsch E, Bühlmann P, Badertscher M (2009) Structure determination of organic compounds, tables of spectral data, 4th revised and enlarged edition. Springer, Berlin
37. Kryszak D, Stawicka K, Calvino-Casilda V, Martin-Aranda R, Ziolek M (2017) Appl Catal A 531:139
38. Calvino-Casilda V, Olejniczak M, Martin-Aranda RM, Ziolek M (2016) Microporous Mesoporous Mater 224:201
39. Wang L, Wang L, Jin H, Bing N (2011) Catal Commun 15:78
40. Van Dommele S, De Jong KP, Bitter JH (2006) Chem Commun. https://doi.org/10.1039/B610208E